NUMERICAL ASSESSMENT OF RECTANGULAR STRAIGHT/REVERSE MUFFLERS AT HIGH-ORDER-MODES

Y. C. Chang **D. Y. Lin**

Department of Mechanical Engineering
Tatung University
Taipei, Taiwan

H. C. Cheng **M. C. Chiu***

Department of Mechanical and Automation Engineering
Chung Chou University of Science and Technology
Changhua, Taiwan

ABSTRACT

There has been wide-spread use of plane wave theory in muffler design in industry. However, This has led to an underestimation of acoustical performances at higher frequencies. To overcome the above drawback, the finite element and boundary element methods have been developed. Nevertheless, the time consumed in calculating the noise level is unacceptable. Moreover, considering the acoustical effect and necessity of space-constrained situation in industry, a compact design of reverse mufflers which may improve the acoustical efficiency is then proposed.

In this paper, a numerical assessment of rectangular mufflers hybridized with straight/reverse chambers using eigen function, four-pole matrix, and genetic algorithm under limited space is developed. Before the optimization is performed, an accuracy check of the mathematical models for the muffler will be carried out. Results reveal that the noise reduction will increase when the number of chambers increases. In addition, the acoustical performance of the mufflers is reversely proportional to the diameter of the inlet/outlet tubes. Also, the TL of the mufflers will be improved when using more number of target tones in the objective function. Consequently, a successful approach in searching optimal shaped rectangular straight/reverse mufflers using an eigen function and a genetic algorithm method within a constrained space has been demonstrated.

Keywords: Bias, Eigen function, Higher order mode, Optimization, Reverse.

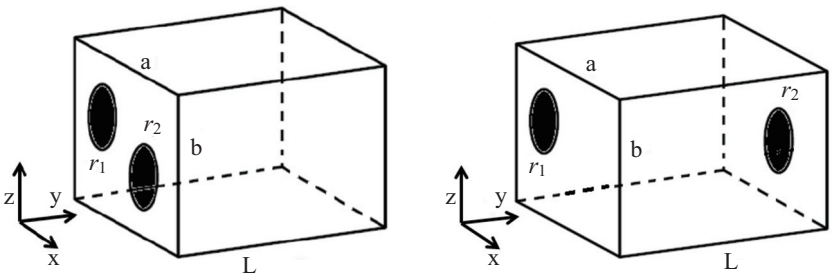
1. INTRODUCTION

Muffler has been widely used in dealing with noise wave emitted from a gas venting equipment. Davis [1], in 1954, started to analyze mufflers and experimentally investigate the wave effect using a plane wave theory. Then, in 1957, based on a fluid dynamic theory, Munjal [2] predicted noise reduction using a four-pole transfer matrix. In 1978-1979, Sullivan and Crocker [3, 4] deduced coupled equations for the outer and the inner tubes of a perforated muffler. However, the acoustical effect of a higher order wave had been neglected. To overcome this drawback, Ih and Lee [5, 6] proposed a theoretical method to predict the acoustical performance of a circular-sectioned expansion muffler. In 1987, Munjal [7] proposed a numerical analysis method to simplify the calculation of an expansion muffler with rectangular and circular sections; however, the ratio of the expansion area to the inlet/outlet area needed to have an integer value. Additionally, the analysis is difficult if the angle between inlet and outlet is 90 degrees. Furthermore, Mimani and Munjal [8] analyzed an elliptical end and expansion-chamber muffler using transverse plane-wave theory. Based on plane wave model, Siano *et al.* [9] explored acoustic performance and fluid-dynamic optimization of an automotive muffler. However, the acoustical effect for a higher order wave was not considered.

In addition, the finite element method [10-18] and the two-dimensional boundary element method [14, 19] have also been used in analyzing the mufflers. They, however, required more calculation time. Ih [20], in 1992, addressing the acoustical effect of a higher order wave,

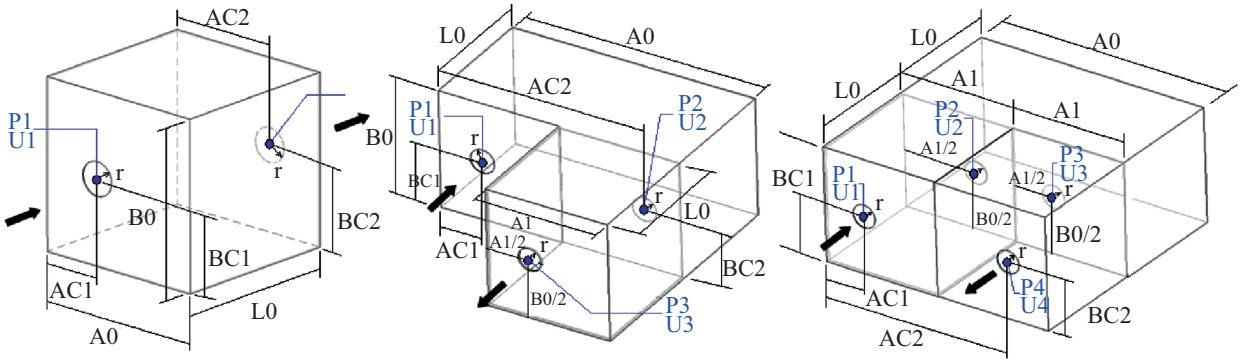
* Corresponding author (minchie.chiu@msa.hinet.net)

DOI : 10.1017/jmech.2016.123
Copyright © 2016 The Society of Theoretical and Applied Mechanics
https://doi.org/10.1017/jmech.2016.123 Published online by Cambridge University Press



(a) Reverse type of rectangular muffler (b) straight type of rectangular muffler

Fig. 1 Single-chamber straight/reverse rectangular mufflers with different allocations of inlets and outlets.



(a) Muffler A (b) Muffler B (c) Muffler C

Fig. 2 Three kinds of rectangular hybrid mufflers (muffler A: a straight muffler equipped with a rectangular chamber; muffler B: a hybrid muffler equipped with a straight rectangular chamber and a reverse rectangular chamber; muffler C: a hybrid muffler equipped with two straight rectangular chambers and a reverse rectangular chamber).

proposed a numerical method for analyzing the acoustical performance of an expansion muffler that was equipped with a circular/rectangular section and an inlet/outlet duct. However, the shape optimization of a space–constrained muffler propagated by the higher order waves was usually ignored. In a previous study, the optimization of an expansion chamber muffler at high-order-mode was discussed [21]. So, in order to enhance the acoustical performance of the muffler within a space-constrained situation, a straight muffler and a reverse muffler with bias inlet/outlet is considered. Here, three kinds of rectangular hybrid mufflers (muffler A: a straight muffler equipped with a rectangular chamber; muffler B: a hybrid muffler equipped with a straight rectangular chamber and a reverse rectangular chamber; muffler C: a hybrid muffler equipped with two straight rectangular chambers and a reverse rectangular chamber) are proposed and optimally shaped using the GA method.

2. THEORETICAL BACKGROUND

First, based on a higher order wave propagation, the mathematical models of single-chamber straight/reverse rectangular mufflers with different allocations of inlets and outlets shown in Fig. 1 are derived below. In order to increase the acoustical performance of the muffler, three kinds of rectangular hybrid mufflers (muffler A: a straight muffler equipped with a rectangular chamber; muffler B: a hybrid muffler equipped with a straight rectangular chamber and a reverse rectangular chamber; muffler C: a hybrid muffler equipped with two straight rectangular chambers and a reverse rectangular chamber) shown in Fig. 2 are proposed.

The three-dimensional governing equation of the sound wave for a single-chamber rectangular muffler is

$$\nabla^2\phi = \left(1/c^2\right)\partial^2\phi/\partial t^2 \tag{1}$$

Assuming the simple harmonic motion of the piston yields

$$\phi(x,y,z,t) = \phi(x,y,z)e^{j\omega t} \tag{2a}$$

where

$$\phi(x,y,z) = \sum_{m=0}^{\infty}\sum_{n=0}^{\infty}\cos\left(\frac{m\pi x}{a}\right)\cos\left(\frac{n\pi z}{b}\right)\left[A_{mn}e^{-jk_y y} + B_{mn}e^{jk_y y}\right] \tag{2b}$$

$$k_x^2 + k_y^2 + k_z^2 = k^2 \tag{2c}$$

https://doi.org/10.1017/jmech.2016.123 Published online by Cambridge University Press

Rearranging Eq. (2c) yields

$$k_y^{\pm} = \mp\sqrt{k^2 - (m\pi/a)^2 - (n\pi/b)^2} = \mp k_y \tag{3}$$

Doing a partial differential to y and setting the boundary condition at $y = L$ yields

$$-\partial\phi/\partial y\big|_{y=L} = 0 \tag{4}$$

where l is the length of the chamber.

This becomes

$$B_{mn} = A_{mn} e^{-2jk_y l} \tag{5}$$

Plugging Eq. (5) into Eq. (2b) yields

$$\phi(x,y,z) = \sum_{m=0}^{\infty}\sum_{n=0}^{\infty} 2A_{mn}\cos\left(\frac{m\pi x}{a}\right)\cos\left(\frac{n\pi z}{b}\right)\cos\{k_y(l-y)\}e^{-jk_y l} \tag{6}$$

Doing a partial differential to y and setting the boundary condition at $y = 0$ yields

$$-\partial\phi/\partial y\big|_{y=0} = V_1 \cdot f(x,y) \tag{7}$$

where V_1 is the average particle velocity and f(x,y) is the step function of 1.

By multiplying the cosine functions of $\int_0^a\int_0^b \cos\frac{m'\pi x}{a}\cos\frac{n'\pi z}{b}dxdz$ at Eq. (7) and doing the integration in the xy domain, Eq. (7) becomes [20]

$$V_1\iint \cos\frac{m'\pi x}{a}\cos\frac{n'\pi z}{b}dxdz = \sum_{m,m'=0}^{\infty}\sum_{n,n'=0}^{\infty} 2A_{mn}\int_0^a\int_0^b \cos\frac{m\pi x}{a}\cos\frac{n\pi z}{b}\cos\frac{m'\pi x}{a}\cos\frac{n'\pi z}{b}dxdz\sin(k_y l)e^{-jk_y l} \tag{8}$$

Concerning a circular section for the inlet and outlet tubes, the velocity potential energy at the piston's inlet is expressed as [20]

$$\phi_1(x,y,z) = -V_1\left\{\begin{array}{l}\dfrac{\pi r_1^2}{ab}\dfrac{\cos k(l-y)}{k\sin kl} \\ +\sum_m{}'\sum_n{}' \dfrac{\pi r_1^2}{ab}\dfrac{2}{v(m,n)}\dfrac{J_1(w(m,n)r_1)}{w(m,n)}\dfrac{1}{k_y\sin k_y l} \\ \quad\times\cos\left(\dfrac{m\pi a_c}{a}\right)\cos\left(\dfrac{n\pi b_c}{b}\right)\cos\left(\dfrac{m\pi x}{a}\right)\cos\left(\dfrac{n\pi z}{b}\right)\cos k_y(l-y)\end{array}\right\} \tag{9a}$$

$$w(m,n) = \{(m\pi/a)^2 + (n\pi/b)^2\}^{1/2} \tag{9b}$$

where J_1 is the first order of the first kind of Bessel function seen as [22] and $v(m, n)$ is the v's come from evaluating equation (l0) of reference 20, where the integration on the right side is a suitable form for the application of the orthogonality of the eigenfunctions.

$$J_{2q}(\xi) = \frac{1}{\pi}\int_0^{\pi}\cos(\xi\sin\theta)\cos 2q\theta d\theta \tag{10}$$

$$\int \eta J_0(\eta)d\eta = \eta J_1(\eta) \tag{11}$$

Assuming a harmonic sound wave propagation, the acoustical pressure at the inlet becomes [20]

$$\begin{aligned} p_1(x,y,z) &= j\omega\rho\phi_1(x,y,z) \\ &= -jU_1Z_0\left\{\frac{\pi r_1^2}{ab}\frac{\cos k(l-y)}{k\sin kl} + \sum_m{}'\sum_n{}'\frac{\pi r_1^2}{ab}\frac{2}{v_{nm}}\frac{J_1(w(m,n)r_1)}{w(m,n)}\frac{1}{k_y\sin k_y l}\right. \\ &\quad\left.\times\cos\left(\frac{m\pi a_c}{a}\right)\cos\left(\frac{n\pi b_c}{b}\right)\cos\left(\frac{m\pi x}{a}\right)\cos\left(\frac{n\pi z}{b}\right)\cos k_y(l-y)\right\} \end{aligned} \tag{12}$$

The average acoustical pressure $\overline{p}_{ih}$ at normal vector of a plane i-h yield [20]

$$\begin{aligned} \overline{p}_{ih} &= (-1)^h jU_1Z_0\left[\frac{1}{\sin kl} + \sum_m{}'\sum_n{}'\frac{4}{v(m,n)}\frac{1}{r_h r_i^2}\frac{k}{k_y\sin k_y l}\frac{J_1(wr_h)J_1(wr_i)}{w^2}\cos\left(\frac{m\pi a_{ch}}{a}\right)\cos\left(\frac{n\pi b_{ch}}{b}\right)\right. \\ &\quad\left.\cos\left(\frac{m\pi a_{ci}}{a}\right)\cos\left(\frac{n\pi b_{ci}}{b}\right)\right] \\ &= (-1)^i jU_iZ_0E_{ih} \end{aligned} \tag{13a}$$

https://doi.org/10.1017/jmech.2016.123 Published online by Cambridge University Press

where

$$i = 1, 2; \quad h = 1, 2 \tag{13b}$$

Concerning a reverse rectangular muffler (inlet and outlet on the same side) shown in Fig. 1(a), the average acoustical pressures at inlet and outlet are $\bar{p}_{11}$ and $\bar{p}_{22}$ where $i = h = 1$ and $i = h = 2$, respectively.

Similarly, for a straight rectangular muffler (inlet and outlet on opposite sides) shown in Fig. 1(b), the average acoustical pressures at inlet and outlet are $\bar{p}_{12}$ and $\bar{p}_{21}$ where (i,h) are (1,2) and (2,1), respectively.

By using the superposition method, the overall potential energy at the chamber inlet is

$$\bar{P}_1 = \bar{p}_{11} + \bar{p}_{12} = -jZ_0\left(U_1E_{11} - U_2E_{12}\right) \tag{14}$$

Similarly, the overall potential energy at the chamber outlet is

$$\bar{P}_2 = \bar{p}_{21} + \bar{p}_{22} = -jZ_0\left(U_1E_{21} - U_2E_{22}\right) \tag{15}$$

The acoustical transfer matrix between nodes 1 and 2 is

$$\begin{bmatrix} P_1 \\ U_1 \end{bmatrix} = \begin{bmatrix} T_{11} & T_{12} \\ T_{21} & T_{22} \end{bmatrix} \begin{bmatrix} P_2 \\ U_2 \end{bmatrix} \tag{16}$$

Developing Eq. (16) yields

$$P_1 = T_{11}P_2 + T_{12}U_2 \tag{17a}$$

$$U_1 = T_{21}P_2 + T_{22}U_2 \tag{17b}$$

where

$$\begin{aligned} T_{11} &= \left(\bar{P}_1 / \bar{P}_2\right)\Big|_{U_2=0} = E_{11}/E_{12}, \\ T_{12} &= \left(\bar{P}_1 / U_2\right)\Big|_{\bar{P}_2=0} = jZ_0\left(E_{12} - E_{11}E_{22}/E_{12}\right) \\ T_{21} &= \left(U_1 / \bar{P}_2\right)\Big|_{U_2=0} = j\left(Z_0E_{12}\right)^{-1}, \\ T_{22} &= \left(U_1 / U_2\right)\Big|_{\bar{P}_2=0} = E_{22}/E_{12} \end{aligned} \tag{17c}$$

Consequently, the transmission loss (TL) of the muffler is

$$TL = 20\log\left[\frac{\left|T_{11} + \frac{T_{12}}{Z_2} + T_{21}Z_1 + T_{22}(S_2/S_1)\right|}{2}\right] \tag{18a}$$

where

$$\begin{aligned} &Z_1 = \rho_0 c / S_1; \quad Z_2 = \rho_0 c / S_2; \\ &S_1 = \pi r_1^2; \quad S_2 = \pi r_2^2 \end{aligned} \tag{18b}$$

Based on above derivations, the acoustical performance of mufflers A-C shown in Fig. 2 will be established as follows:

For the i-th muffler (muffler A: $i = 1$; muffler B: $i = 2$; muffler C: $i = 3$), the system's four-pole matrix and TL are

$$\begin{aligned} \begin{bmatrix} P_1 \\ U_1 \end{bmatrix} &= \prod_{m=1}^{element_i[muffler_i]} \left[T_m(f)\right] \begin{bmatrix} P_{element_{i+1}} \\ U_{element_{i+1}} \end{bmatrix} \\ &= \begin{bmatrix} T_{T11} & T_{T12} \\ T_{T21} & T_{T22} \end{bmatrix} \begin{bmatrix} P_{element_{i+1}} \\ U_{element_{i+1}} \end{bmatrix} \end{aligned} \tag{19a}$$

$$TL_i(f, \bar{X}_i) = 20\log\left[\frac{\left|T_{T11} + \frac{T_{T12}}{Z_2} + T_{T21}Z_1 + T_{T22}(S_{element_i+1}/S_1)\right|}{2}\right] \tag{19b}$$

where

$$\begin{aligned} &i = 1 \text{ to } 3; \quad X_i = (r, AC_1, AC_2); \\ &element_1 = 2; \quad element_2 = 3; \quad element_3 = 4 \end{aligned} \tag{19c}$$

Three kinds of multi-tone optimizations (case 1: one tone of 1000 Hz; case 2: two tones of 1000 Hz and 1500 Hz; case 3: three tones of 500 Hz, 1000 Hz, and 1500 Hz) are considered for use in mufflers A-C.

By using the formulas of Eq. (19), the objective functions used in the GA optimization with respect to each type of mufflers are established. For the i-th muffler (i = 1 for muffler A, i = 2 for muffler B, and i = 3 for muffler C), the objective function in maximizing the *STL* at the k-th case (k = 1 to kk) is

$$OBJ_{ik} = \sum_{k=1}^{kk}\left[TL_i(f_k, \bar{X}_i)\right] / kk \tag{20}$$

where i = 1-3, kk = 1-3, $f_{k=1}$ = 1000 Hz, $f_{k=2}$ = 1500 Hz, and $f_{k=3}$ = 500 Hz.

3. MODEL CHECK

Before performing the *GA* optimal simulation on rectangular mufflers, an accuracy check of the mathematical model for a single-chamber rectangular straight muffler equipped with bias inlet/outlet tube at muffler length (C) of 0.1 M and 0.3 M is verified using Abom *et al*. data [23]. Results in Fig. 3 reveal that they are in agreement. Consequently, the models linked with the numerical method are applied in the shape optimization of mufflers A-C shown in Fig. 2 in the following section.

4. SENSITIVITY ANALYSIS

Before the related design parameters of mufflers A-C are selected, the sensitivity analysis of sound transmission loss with respect to various geometric parameters is required. The related geometric parameters of a single-chamber rectangular straight muffler and a single-chamber rectangular reverse muffler are shown in Figs. 4(a) and 4(b). The sensitivity analysis of a single-chamber

https://doi.org/10.1017/jmech.2016.123 Published online by Cambridge University Press

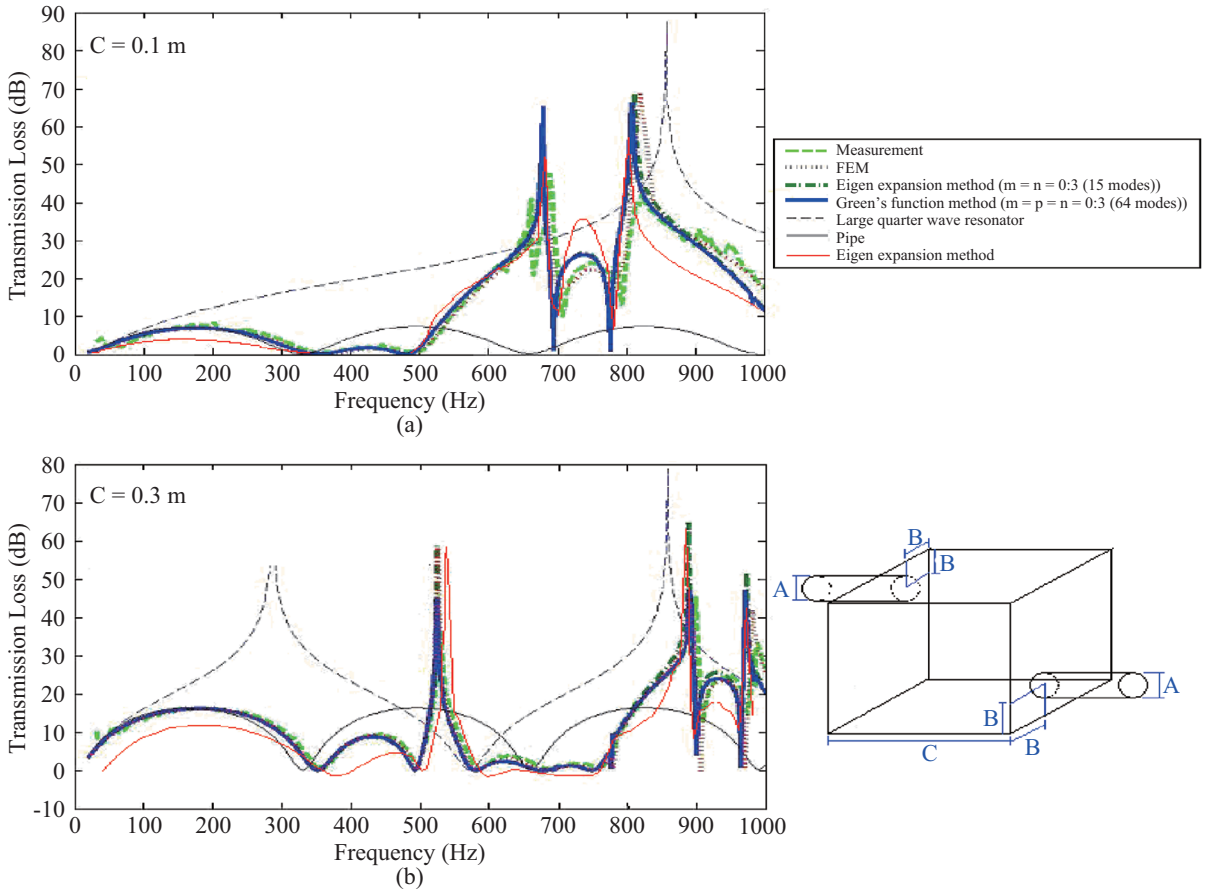
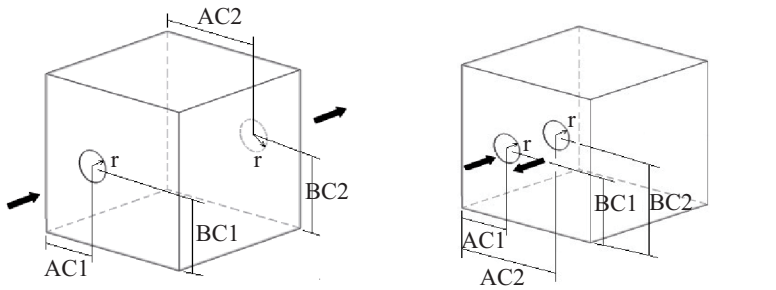


Fig. 3 Accuracy check of a single-chamber rectangular straight muffler equipped with a bias inlet/outlet tube using Abom *et al*. data (a: C = 0.1 m; b: C = 0.3 m) [23].



(a) A single-chamber straight muffler (b) A single-chamber reverse muffler

Fig. 4 Geometric parameters of a single-chamber rectangular straight muffler and a single-chamber rectangular reverse muffler.

straight rectangular muffler by varying the locations of the inlet tube (AC1) and the outlet tube (AC2) is depicted in Fig. 5. Similarly, the related sensitivity analysis of a single-chamber straight rectangular muffler by varying the radius (r) of the inlet tube and the outlet tube is plotted in Fig. 6. As indicated in Figs. 5-6, the sound transmission loss of the single-chamber straight rectangular muffler is very sensitive when the geometric parameters of AC1, AC2, and r are varied. As can be seen in Figs. 5-6, the bias of inlet/outlet tubes and the radius of inlet/outlet tubes play essential roles in the acoustical performance. Therefore, three geometric parameters of AC1, AC2, and r are selected as the design parameters in the shape optimization process of reverse rectangular mufflers.

The related sensitivity analysis of a single-chamber reverse rectangular muffler by varying the locations of inlet tube (AC1) and outlet tube (AC2) is depicted in Fig. 7. Similarly, the related sensitivity analysis of a single-chamber straight rectangular muffler by varying the radius (r) of inlet tube and outlet tube is plotted in Fig. 8. As indicated in Figs. 7-8, the sound transmission

https://doi.org/10.1017/jmech.2016.123 Published online by Cambridge University Press

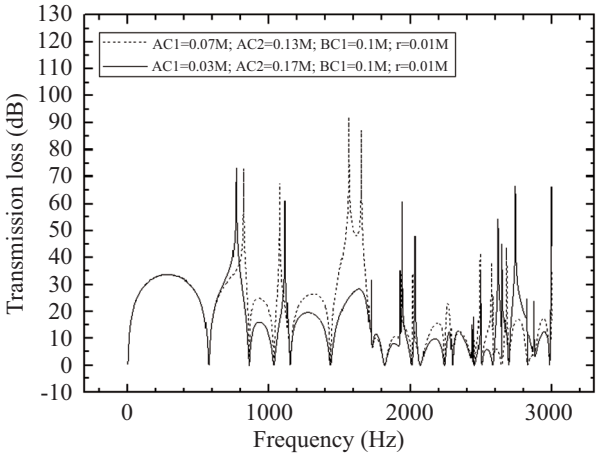


Fig. 5 The sensitivity analysis of a single-chamber straight rectangular muffler when varying the geometric parameter of AC1 and AC2 (geometry is shown in Fig. 4(a)).

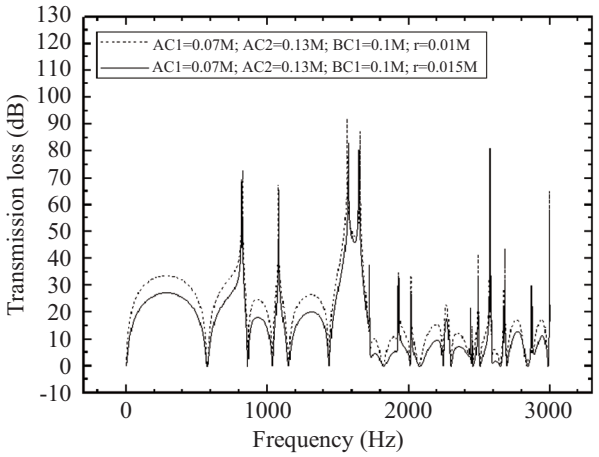


Fig. 6 The sensitivity analysis of a single-chamber straight rectangular muffler when varying the geometric parameter of r (geometry is shown in Fig. 4(a)).

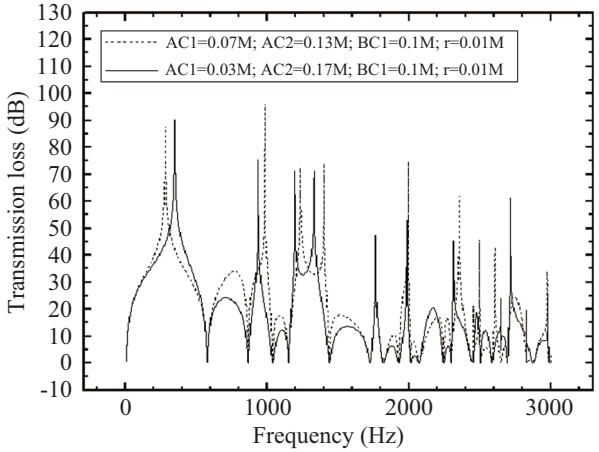


Fig. 7 The sensitivity analysis of a single-chamber reverse rectangular muffler when varying the geometric parameter of AC1 and AC2 (geometry is shown in Fig. 4(b)).

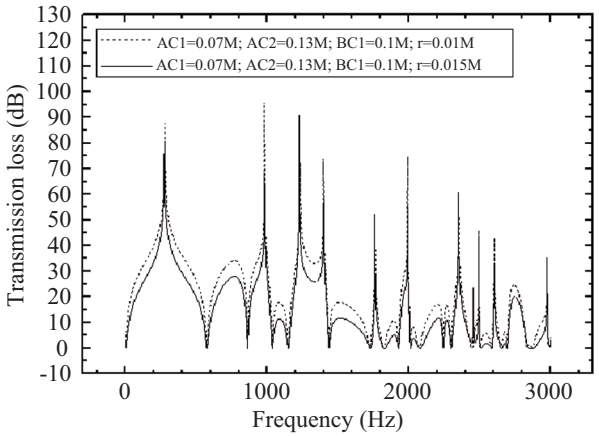


Fig. 8 The sensitivity analysis of a single-chamber reverse rectangular muffler when varying the geometric parameter of r (geometry is shown in Fig. 4(b)).

loss of the single-chamber reverse rectangular muffler is very sensitive when the geometric parameters of AC1, AC2, and r are varied. As can be seen in Figs. 7-8, the bias of inlet/outlet tubes and the radius of inlet/outlet tubes play essential roles in the acoustical performance. Therefore, three geometric parameters of AC1, AC2, and r are selected as the design parameters during the shape optimization process of reverse rectangular mufflers.

Based on the sensitivity analysis mentioned above, the designed parameters ($\overline{X}_1, \overline{X}_2, \overline{X}_3$) of muffler A, muffler B, and muffler C shown in Fig. 2, are then selected and depicted in Eq. (19).

5. GENETIC ALGORITHM

A Genetic Algorithm (*GA*), one kind of evolutionary algorithm used to search for the global optimum by imitating a genetic evolutionary process, was invented by Holland [24] and developed to functional optimization by De Jong [25]. It has been widely used in various fields [26-30]. The GA operation is shown in Fig. 9. Here, the tournament selection, a random comparison of the relative fitness from pairs of chromosomes, was adopted and applied in the gene's elitism process. In addition, uniform crossover was used as a gene's crossover where one pair of offspring from the selected parent was generated with a probability of *pc*. Note that a mutation occurred with a probability of *pm* where the new and unexpected point was applied to the *GA* optimizer's search domain.

Consequently, as indicated in Fig. 10, the process will be terminated if the number of generations reaches a pre-selected value of $iter_{\max}$.

https://doi.org/10.1017/jmech.2016.123 Published online by Cambridge University Press

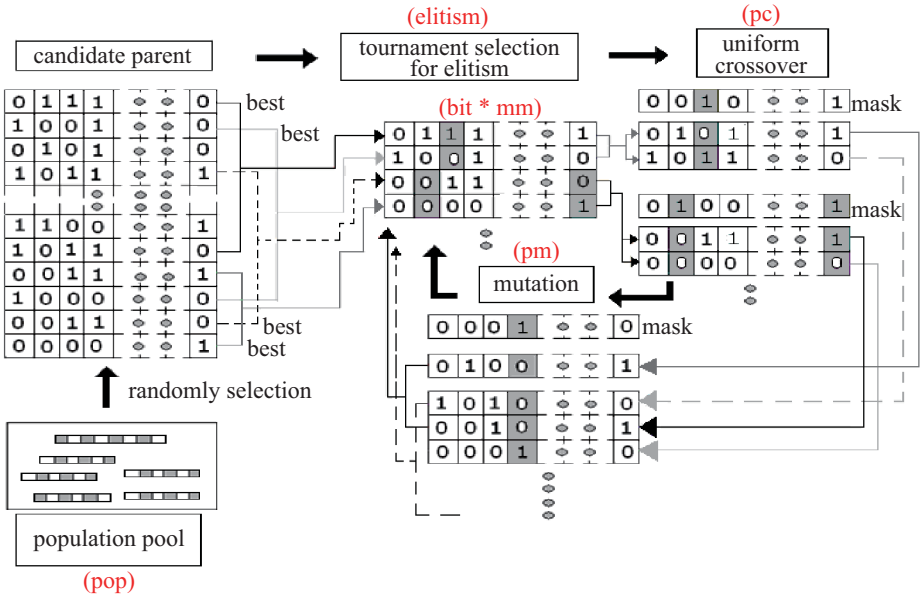


Fig. 9 Operations of the *GA* method.

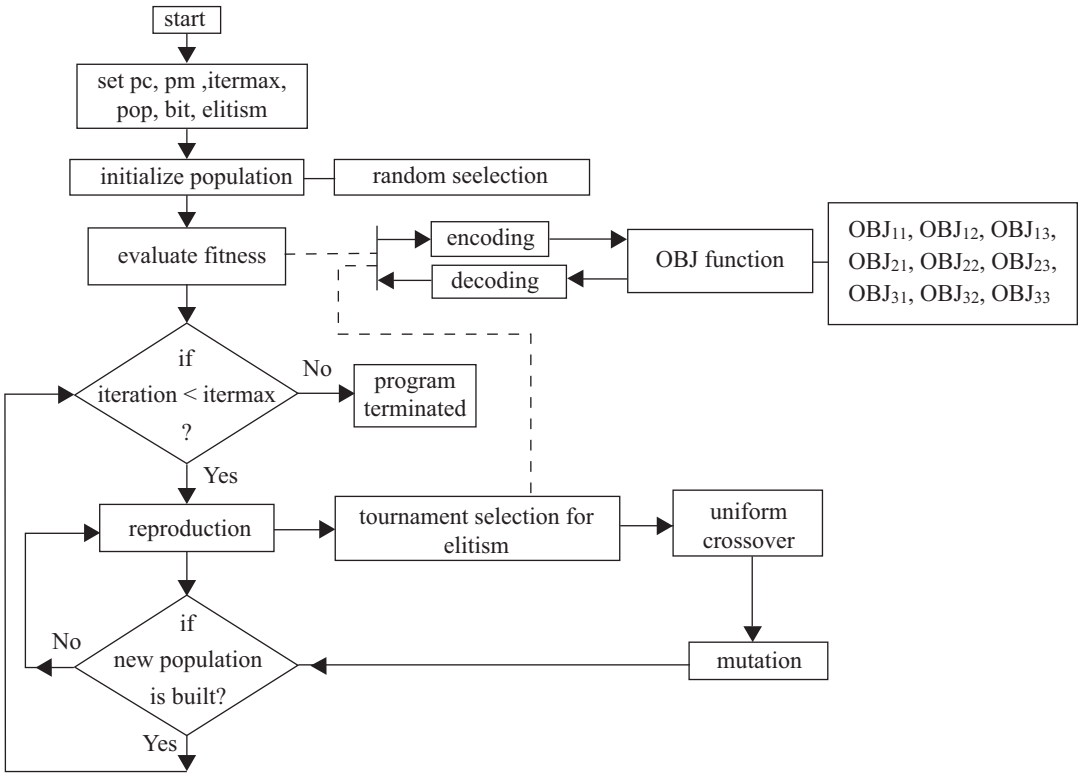


Fig. 10 Flow diagram for the *GA* method.

6. RESULTS AND DISCUSSION

6.1 Results

The *GA* control parameters include *pop* (population number), *bit* (chromosome length), *pc* (crossover rate), *pm* (mutation factor), and $iter_{max}$ (maximum iteration). To achieve a good optimization, five control parameters are varied step by step. The related *GA* control parameters used in the optimization are shown in Table 1.

Utilizing Eq. (20) and using the *GA* parameters in the optimization process, the optimal design data of muffler A with respect to cases 1-3 was performed and shown in Table 2. The related maximizations of the TL_1 with respect to cases 1-3 are depicted in Tables 3-5. Using the design data in the theoretical calculation, the related *TL* spectrum of muffler A with respect to case 1 (targeted tone of 1000 Hz) is plotted in Fig. 11. A comparison of the *TL* for three cases is also illustrated in Fig. 12.

https://doi.org/10.1017/jmech.2016.123 Published online by Cambridge University Press

Table 1 Selected GA parameters during shape optimization

GA parameters	Value (or condition)
bit	20
pop	50
elitism	(tournament)
crossover	(uniform crossover)
pc	0.5
pm	0.5
$iter_{max}$	1000

Table 2 Optimal design parameters with respect to three kinds of optimization cases (muffler A).

Muffler A	r (m)	AC1 (m)	AC2 (m)
case 1	0.0018	0.0626	0.0528
case 2	0.0013	0.0828	0.0101
case 3	0.0012	0.0421	0.0343
Note: A0 = 0.10 m; B0 = 0.10 m; L0 = 0.20 m; BC1 = 0.05 m; BC2 = 0.05 m			

Table 3 Optimal design parameters for muffler A (case 1)

Case 1	Targeted tone
	1000 Hz
Original TL1 (before optimization) – dB	27.4
Optimal TL1 (after optimization) – dB	47
Improvement – dB	19.6

Table 4 Optimal design parameters for muffler A (case 2)

Case 2	Targeted tones	
	1000 Hz	1500 Hz
Original TL1 (before optimization) – dB	27.4	29
Optimal TL1 (after optimization) – dB	62.3	64
improvement	34.9	35

Table 5 Optimal design parameters for muffler A (case 3)

Case 3	Targeted tones		
	500 Hz	1000 Hz	1500 Hz
Original TL1 (before optimization) – dB	33.5	27.4	29
Optimal TL1 (after optimization) – dB	81.4	73.3	62.2
Improvement – dB	47.9	45.9	33.2

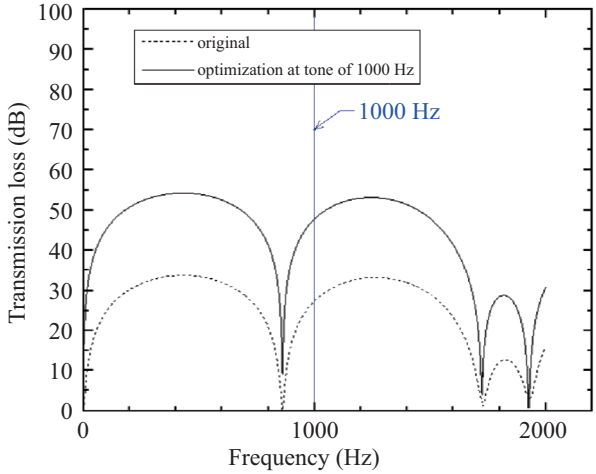


Fig. 11 Comparison of sound transmission loss before and after the optimization is performed (muffler A at case 1 (targeted tone of 1000 Hz)).

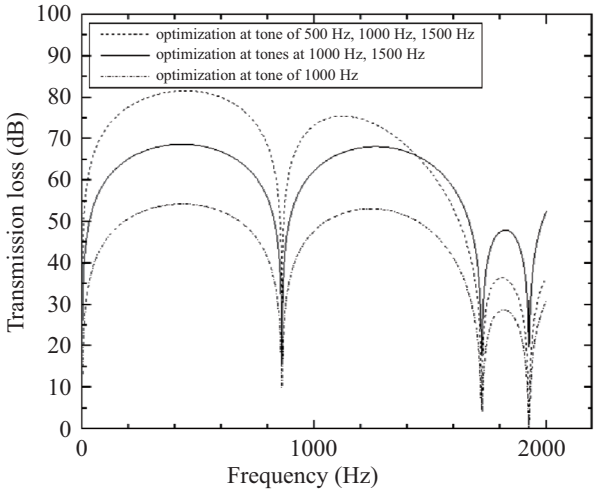


Fig. 12 Comparison of the optimal sound transmission loss for three cases (muffler A).

Similarly, utilizing Eq. (20) and using the *GA* parameters in the muffler B's optimization process, the optimal design data with respect to cases 1-3 was performed and shown in Table 6. The related maximizations of the TL_2 with respect to cases 1-3 are depicted in Tables 7-9. Using the design data in the theoretical calculation, the related *TL* spectrum of muffler B with respect to case 2 (targeted tones of 1000 Hz and 1500 Hz) is also illustrated in Fig. 13. In addition, a comparison of the *TL* for the three cases is plotted in Fig. 14.

Table 6 Optimal design parameters with respect to three kinds of optimization cases (muffler B).

Muffler B	r (m)	AC1 (m)	AC2 (m)
case 1	0.0014	0.0211	0.0885
case 2	0.0016	0.0297	0.0909
case 3	0.0015	0.0852	0.0107
Note: A0 = 0.20 m; B0 = 0.10 m; L0 = 0.20 m; BC1 = 0.05 m; BC2 = 0.05 m			

https://doi.org/10.1017/jmech.2016.123 Published online by Cambridge University Press

Table 7 Optimal design parameters for muffler B (case 1)

Case 1	Targeted tone
	1000 Hz
Original TL2 (before optimization) – dB	52.2
Optimal TL2 (after optimization) – dB	84.1
Improvement – dB	31.9

Table 8 Optimal design parameters for muffler B (case 2)

Case 2	Targeted tones	
	1000 Hz	1500 Hz
Original TL2 (before optimization) – dB	52.2	50.8
Optimal TL2 (after optimization) – dB	57.4	62.8
Improvement – dB	5.2	12

Table 9 Optimal design parameters for muffler B (case 3)

Case 3	Targeted tones		
	500 Hz	1000 Hz	1500 Hz
Original TL2 (before optimization) – dB	93.8	52.2	50.8
Optimal TL2 (after optimization) – dB	70.2	61.4	65.7
Improvement – dB	-23.6	9.2	14.9

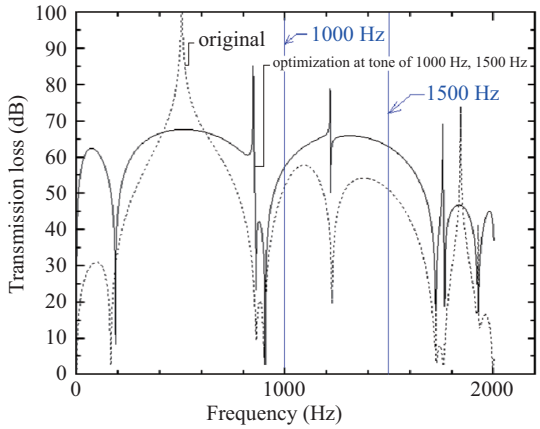


Fig. 13 Comparison of the sound transmission loss before and after the optimization is performed (muffler B at case 2 (targeted tones of 1000 Hz and 1500 Hz)).

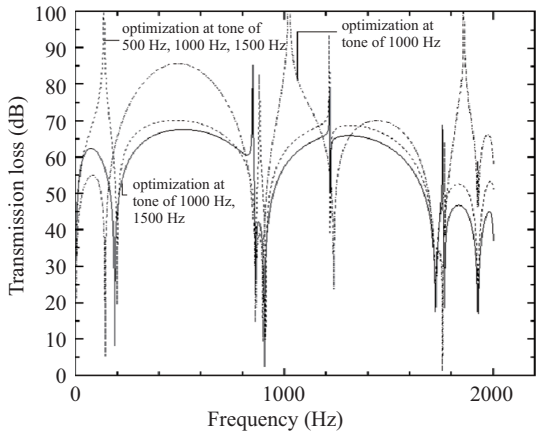


Fig. 14 Comparison of the optimal sound transmission loss for three cases (muffler B).

Utilizing Eq. (20) and using the *GA* parameters in muffler C's optimization process, the optimal design data with respect to cases 1-3 was performed and shown in Table 10. The related maximizations of the TL_3 with respect to cases 1-3 are depicted in Tables 11-13. Using the design data in the theoretical calculation, the related *TL* spectrum of muffler C with respect to case 3 (targeted tones of 500 Hz, 1000 Hz, and 1500 Hz) is shown in Fig. 15. Furthermore, a comparison of the *TL* for the three cases is plotted in Fig. 16.

Table 10 Optimal design parameters with respect to three kinds of optimization cases (muffler C)

Muffler C	r (m)	AC1 (m)	AC2 (m)
case 1	0.0010	0.0247	0.0136
case 2	0.0011	0.0361	0.0742
case 3	0.0014	0.0582	0.0637
Note: A0 = 0.20 m; B0 = 0.10 m; L0 = 0.20 m; BC1 = 0.05 m; BC2 = 0.05 m			

Table 11 Optimal design parameters for muffler C (case 1)

case C	Targeted tone
	1000 Hz
Original TL3 (before optimization) – dB	48.6
Optimal TL3 (after optimization) – dB	76
Improvement – dB	27.4

Table 12 Optimal design parameters for muffler C (case 2)

case B	Targeted tones	
	1000 Hz	1500 Hz
Original TL3 (before optimization) – dB	48.6	73
Optimal TL3 (after optimization) – dB	30.8	91
Improvement – dB	-17.8	18

Table 13 Optimal design parameters for muffler C (case 3)

case A	Targeted tones		
	500 Hz	1000 Hz	1500 Hz
Original TL3 (before optimization) – dB	65	48.6	73
Optimal TL3 (after optimization) – dB	92.4	84.9	90.5
Improvement – dB	27.4	36.3	17.5

https://doi.org/10.1017/jmech.2016.123 Published online by Cambridge University Press

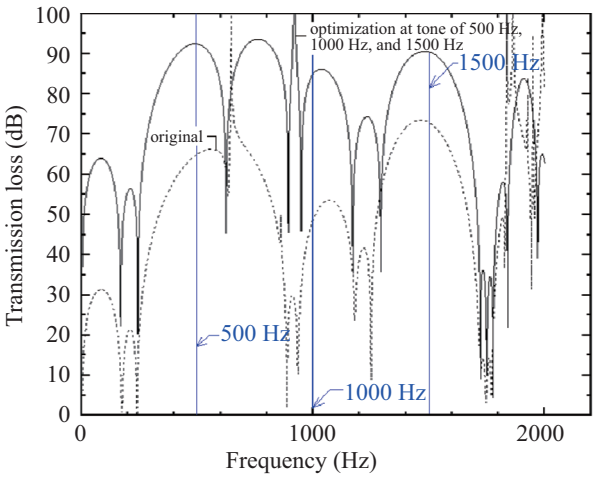


Fig. 15 Comparison of the sound transmission loss before and after the optimization is performed (muffler C at case 3 (targeted tones of 500 Hz, 1000 Hz, and 1500 Hz)).

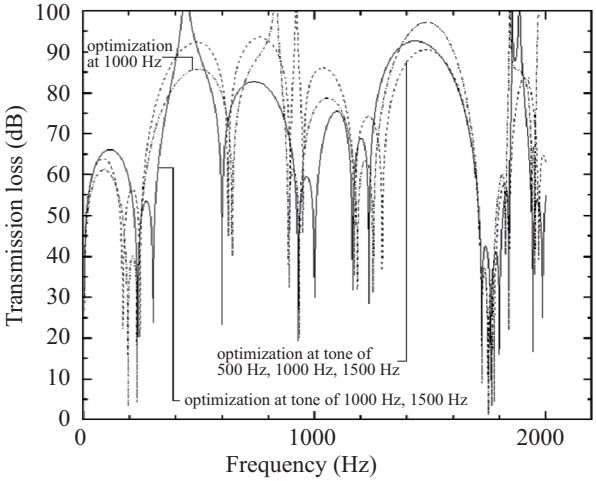


Fig. 16 Comparison of the optimal sound transmission loss for three cases (muffler C).

6.2 Discussion

As indicated in Tables 3-5 and Figs. 11-12, the broadband *TL* of muffler A is largely improved if the number of target tones increases. Results in case 1 reveal that the improvement of noise reduction with respect to 1000 Hz reaches 19.6 dB after the optimization being performed using a target tone of 1000 Hz. Also, results in case 2 demonstrate that the improvement of noise reduction with respect to 1000 Hz and 1500 Hz reaches 34.9 dB and 35.0 dB when using two target tones of 1000 Hz and 1500 Hz. Furthermore, results in case 3 illustrate that the improvement of noise reduction with respect to 500 Hz, 1000 Hz, and 1500 Hz will reach 47.9 dB, 45.9 dB and 33.2 dB when using three target tones of 500 Hz, 1000 Hz and 1500 Hz.

Similarly, as illustrated in Tables 7-9 and Figs. 13-14, concerning muffler B, the profile of *TL* is also improved if the number of target tones increases. Results in case 1 reveal that the improvement of noise reduction with respect to 1000 Hz reaches 31.9 dB after the optimization being performed using a target tone of 1000 Hz. In addition, results in case 2 demonstrate that the improvement of noise reduction with respect to 1000 Hz and 1500 Hz will reach 5.2 -12.0 dB when using these two target tones. Also, results in case 3 illustrate that the improvement of noise reduction with respect to 500 Hz, 1000 Hz, and 1500 Hz will reach -23-15 dB when using three target tones. Furthermore, as illustrated in Tables 11-13 and Figs. 15-16, the broadband *TL* in muffler C is also improved if the number of target tones increases. Results in case 1 also demonstrate that the improvement of noise reduction with respect to 1000 Hz reaches 27.4 dB when using a target tone of 1000 Hz. Results in case 2 demonstrate that the improvement of noise reduction with respect to 1000 Hz and 1500 Hz can reach -17-18.0 dB when using these two target tones. Additionally, results in case 3 illustrate that the improvement of noise reduction with respect to 500 Hz, 1000 Hz, and 1500 Hz will reach 17-36 dB when using three target tones.

As discussed above, the results in case 2 (two target tones) and case 3 (three target tones) reveal that the whole *TL* profile will be promoted when average *TL* of the multiple tones is regarded as the objective function. Moreover, as can be seen in Figs. 12, 14, and 16, the whole *TL* curve in muffler C (a hybrid muffler with three chambers) is superior to other mufflers. This indicates that the broadband *TL* will increase if the number of the muffler's chamber increases. On the contrary, because of the fewest number of chambers, the whole *TL* curve in muffler A is inferior to other mufflers.

7. CONCLUSIONS

It has been shown that the high-order-mode optimization of mufflers can be easily and efficiently carried out by using a four-pole transfer matrix as well as a *GA* optimizer. Results in section 4 demonstrate that the radius and locations of inlet/outlet tubes for a single-chamber straight rectangular muffler and a single-chamber reverse rectangular muffler are sensitive design parameters for the muffler's acoustical performance. In addition, results from various objective functions indicate that the broadband *TL* will be promoted if the number of the target tones used in the objective function increases. Moreover, result in section 6 reveals that the broadband *TL* will increase when the number of chamber increases; however, the backpressure of the muffler will increase, accordingly. Therefore, a compromise between the acoustical performance and backpressure is compulsory if the pressure drop is too big enough to interfere with the system's venting (such as the diesel engine exhaust).

Currently, the mathematical model used in the paper does not consider the influence of acoustical influence with respect to flow, heat, and gas composition. Nevertheless, an effort to include these parameters into the mathematical model in future work is possible. As a viewpoint of fluid dynamic, because secondary noise generated from flowing fluid is tightly related to the passing velocity, a low speed design inside the muffler is

https://doi.org/10.1017/jmech.2016.123 Published online by Cambridge University Press

essential. Therefore, for a muffler constrained within a fixed space, the rectangular shape with the largest cross-section area (compared to other shapes of circular, elliptic, etc.) is then considered and adopted in this paper. Besides, various shapes of mufflers also will influence muffler's acoustical efficiency. The assessment and comparison of different shapes of mufflers will be planned in further work, too.

Consequently, considering the higher order mode of sound wave, the approach used for shape optimization of the hybrid mufflers using multi-tone objective functions is quite important and can be efficiently achieved.

ACKNOWLEDGEMENTS

The authors acknowledge the financial support of Ministry of Science and Technology (MOST 104-2221-E-036-027, ROC).

NOMENCLATURE

AC1	horizontal displacement of the inlet tube (m);
AC2	horizontal displacement of the outlet tube (m);
a_{ci}, a_{ch}	horizontal displacements of the planes (pistons) i and h (m);
b_{ci}, b_{ch}	vertical displacements of the planes (pistons) i and h (m)
b	width of a single-chamber rectangular muffler (m);
Bit	length of the chromosome;
BC1	vertical displacement of the inlet tube (m);
BC2	vertical displacement of the outlet tube (m);
c_0	sound speed (m/s);
f	frequency (Hz);
f(x,y)	step function;
h	height of a single-chamber rectangular muffler (m);
$iter_{\max}$	maximum iteration during GA optimization;
k	wave number of sound wave (ω/c_o).
k_x	wave number of sound wave in x-axis ($m\pi/a$);
k_y	wave number of sound wave in y-axis (nπ/b);
k_z	wave number of sound wave in z-axis $\sqrt{k^2-k_x^2-k_z^2}$;
L	width of a single-chamber rectangular muffler (m);
m, n	acoustical mode;
Mm	number of the design parameters;
$\overline{p}_{ii}$	averaged acoustical pressure (Pa);
$\overline{p}_{i'i}$	averaged interactive acoustical pressure (Pa);
$\overline{P}_1$	acoustical potential energy in the inlet;
$\overline{P}_2$	acoustical potential energy in the outlet;
pc	crossover ratio;
pm	mutation ratio;
pop	number of population;
R, r_1, r_2	radius of the tube (m);
S_0	section area of the expansion chamber (m^2);
S_1	section area of inlet (m^2);
S_2	section area of outlet (m^2);
TL	transmission loss (dB);
U_i	volume velocity (m/s);
V_1	average particle velocity (m/s);
Z_0	acoustical impedance of the expansion chamber in z-axis;
ω	angular frequency (= $2\pi f$) (rad/s);
ρ_0	air density (kg/m^3);

REFERENCES

1. Davis, D. D., Stokes, J. M., Moore, D. and Steven, L., "Theoretical and Experimental Investigation of Mufflers with Comments on Engine Exhaust Muffler Design," *NACA Report 1192* (1954).
2. Munjal, M. L., "Velocity Ratio-cum-transfer Matrix Method for the Evaluation of a Muffler with Mean Flow," *Journal of the Acoustical Society of America,* **39**, pp. 105-119 (1957).
3. Sullivan, J. W. and Crocker, M. J., "Analysis of Concentric-tube Resonators Having Unpartitioned Cavities," *Journal of the Acoustical Society of America*, **64**, pp. 207-215 (1978).
4. Sullivan, J. W., "A Method for Modeling Perforated Tube Muffler Components. I: Theory," *Journal of the Acoustical Society of America*, **66**, pp. 772-778 (1979).
5. Ih, J. G. and Lee, B. H., "Analysis of Higher-order Mode Effects in the Circular Expansion Chamber with Mean Flow," *Journal of the Acoustical Society of America*, **77**, pp. 1377-1388 (1985).
6. Ih, J. G. and Lee, B. H., "Theoretical Prediction of the Transmission Loss of Circular Reversing Chamber Mufflers," *Journal of Sound and Vibration*, **112**, pp. 261-272 (1987).
7. Munjal, M. L., "A Simple Numerical Method for Three-dimensional Analysis of Simple Expansion Chamber Mufflers of Rectangular as Well as Circular Cross-section with a Stationary Medium," *Journal of Sound and Vibration*, **116**, pp. 71-88 (1987).
8. Mimani, A. and Munjal, M. L., "Transverse Plane-Wave Analysis of Short Elliptical End-Chamber and Expansion-Chamber Mufflers," *International Journal of Acoustics and Vibration*, **15**, pp. 24-38 (2010).
9. Siano, D., Bozza, F. and Auriemma, F., "Acoustic and Fluid-dynamic Optimization of an Automotive Muffler," *Proceedings of the Institution of Mechanical Engineers, Part D: Journal of Automobile Engineering*, **227**, pp. 735-747 (2013).
10. Young, C. I. and Crocker, M. J., "Prediction of Transmission Loss in Mufflers by the Finite-element

https://doi.org/10.1017/jmech.2016.123 Published online by Cambridge University Press

Method," *Journal of the Acoustical Society of America*, **57**, pp. 144-148 (1975).

11. Siano, D., "Three-dimensional/One-dimensional Numerical Correlation Study of a Three-pass Perforated Tube," *Simulation Modelling Practice and Theory*, **19**, pp. 1143-1153 (2011).
12. Siano, D., Auriemma, F. and Bozza, F., "Pros and Cons of Using Different Numerical Techniques for Transmission Loss Evaluation of a Small Engine Muffler," *SAE Technical Paper*, DOI: 10.4271/2010-32-0028 (2010).
13. Jones, P. W. and Kessissoglou, N. J., "A Numerical and Experimental Study of the Transmission Loss of Mufflers used in Respiratory Medical Devices," *Acoustics Australia*, **38**, pp. 13-19 (2010).
14. Ji, Z. and Fang, Z., "Three-pass Perforated Tube Muffler with End-resonator," *SAE International Journal of Passenger Cars - Mechanical Systems*, **4**, pp. 989-999 (2011).
15. Vasile, O. and Gillich, N., "Finite Element Analysis for Reactive and Dissipative Rectangular Muffler," *Recent Advances in Signal Processing, Computational Geometry and Systems Theory*, pp. 251-255 (2011).
16. Reddy, M. R. and Reddy, K. M., "Design and Optimization of Exhaust Muffler in Automobiles," *International Journal of Engineering Research and Applications*, **2**, pp. 395-398 (2012).
17. Vasile, O. and Gillich, G. R., "Finite Element Analysis of Acoustic Pressure Levels and Transmission Loss of a Muffler," *Advances in Remote Sensing, Finite Differences and Information Security*, pp. 43-48 (2012).
18. Jadhav, M. B. and Bhattu, A. P., "Validation of the Experimental Setup for the Determination of Transmission Loss of Known Reactive Muffler Model by Using Finite Element Method," *International Journal of Engineering and Innovative Technology*, **2**, pp. 96-100 (2012).
19. Seybert, A. F. and Cheng, C. Y. R., "Application of the Boundary Element Method to Acoustic Cavity Response and Muffler Analysis," *Transactions of the American Society of Mechanical Engineers, Journal of Vibration, Stress, and Reliability in Design*, **109**, pp. 15-21 (1987).
20. Ih, J. G., "The Reactive Attenuation of Rectangular Plenum Chambers," *Journal of Sound and Vibration*, **157**, pp. 93-122 (1992).
21. Chiu, M. C. and Chang, Y. C., "An Assessment of High-order-mode Analysis and Shape Optimization of Expansion Chamber Mufflers," *Archives of Acoustics*, **39**, pp. 1-11 (2014).
22. Abramowitz, M. and Stegun, I.A., *Mathematical Handbook Handbook of Mathematical Functions: With Formulas, Graphs, and Mathematical Tables*, National Bureau of Standards, Washington (1964).
23. Abom, M. and Qazizadeh, A, "Analytical and Numerical Analysis of the Acoustics of Shallow Flow Reversal Chambers," M.S. Thesis, KTH The Marcus Wallenberg Laboratory for Sound and Vibration Research, Stockholm, Sweden (2012).
24. Holland, J.H., *Adaptation in Natural and Artificial System*, MIT Press Cambridge, MA, USA (1992).
25. De Jong, K. A., "An Analysis of the Behavior of a Class of Genetic Adaptive Systems," Ph.D. Dissertation, University of Michigan, Ann Arbor, Michigan, U.S. (1975).
26. Yeh, L. J., Chang, Y. C., Chiu, M. C. and Lai, G. J., "GA Optimization on Multi-segments Muffler under Space Constraints," *Applied Acoustics*, **65**, pp. 521-543 (2004).
27. Chang, Y. C., Yeh, L. J. and Chiu, M. C., "Optimization of Constrained Multi-layer Absorbers by Using Genetic Algorithms," *International Journal of Acoustics and Vibration*, **9**, pp. 175-185 (2004).
28. Lan, T. S. and Chiu, M. C., "Identification of Noise Sources in Factory's Sound Field by Using Genetic Algorithm," *Applied Acoustics*, **69**, pp. 733-750 (2008).
29. Chiu, M. C., "The Numerical Assessment of Optimal Equipment Allocation and Acoustical Barrier Shape in a Multi-noise Plant by Using the Genetic Algorithm method," *Journal of Marine Science and Technology*, **18**, pp. 56-68 (2010).
30. Chiu, M. C., "Numerical Assessment of Path-planning for an Autonomous Robot Passing through Multi-layer Barrier Systems Using a Genetic Algorithm," *Information Technology Journal*, **9**, pp. 1483-1489 (2010).

(Manuscript received September 11, 2016,
accepted for publication November 10, 2016.)

https://doi.org/10.1017/jmech.2016.123 Published online by Cambridge University Press